Clay mineral solubility from aqueous equilibrium: Assessment of the measured thermodynamic properties

Stéphane Gaboreau, Hélène Gailhanou, Philippe Blanc, Ph Vieillard, B. Madé

Clay mineral solubility from aqueous equilibrium: assessment of the measured thermodynamic properties

S. Gaboreau[1†], H. Gailhanou[1], Ph. Blanc[1], Ph. Vieillard[2], B. Made[3]

[1] BRGM, 3 Avenue Claude Guillemin, BP6009, F-45060 Orleans, France

[2] CNRS-IC2MP-UMR-7285 -Hydrasa, 5 Avenue Albert Turpain, F-86022 Poitiers Cedex, France

[3]Andra, F-92298 Châtenay-Malabry Cedex, France.

[†] Corresponding author: stephane.gaboreau@brgm.fr

Abstract

Clay minerals (kaolinite KGa-2, smectite MX-80, illite IMt-2, vermiculite SO and Chlorite Cca-2) were equilibrated in aqueous media during long-term batch experiments up to seven years. Dissolved element concentrations were measured, allowing calculation of the ionic activity product of the minerals. An improved protocol for equilibration has been established to limit evaporation over the seven years of the experiments and to optimize the analytical results accuracy. The protocol could be verified with respect to the solubility of kaolinite. For the other minerals, the equilibrium constants obtained could be compared with the values calculated after calorimetric measurements previously performed on the same samples. The ionic activity products extracted for illite, smectite and, to a lesser extent, vermiculite were found to agree with the values issued from the calorimetric measurements. For chlorite in particular, a discrepancy with calorimetric measurements still remains. This was interpreted in terms of dissolution rates getting slower for this mineral, formed at temperatures higher than 25°C.

Keywords : Clay minerals; solubility; thermodynamic; aqueous equilibrium

1. Introduction

Clay dissolution experiments are a straightforward method for obtaining clay solubility by calculating the ionic activity product (*IAP*). Many clays systems were studied during the last decades in determining the Gibbs free energy of formation. Some pioneers (Aja, 1995; Aja et al., 1991a, b; Devidal et al., 1996; Kittrick, 1966, 1971b; May et al., 1986; Reesman and Keller, 1968) have attempted to determine thermodynamic properties of many clays minerals (kaolinite, illite, smectite, chlorite) from solubility measurements. The principle consists in allowing the mineral to equilibrate within a solution over time and measure the aqueous concentration of constituent elements released into solution. Due to the slow dissolution rate of clay minerals (Cama et al., 2000; Devidal et al., 1997; Lasaga, 1998; Marty et al., 2011; Oelkers et al., 1994), which even decreases close to equilibrium, these experiments are conducted over long period of times (several years).

In addition to the equilibrium attainment issue, equilibrium experiments may be subject to different pitfalls that could increase the uncertainties on extracted values:

- Determination of the *IAP,* which is calculated according to the aqueous concentrations, is dependent of the chemical composition of the studied material and of its purity. Solubility measurement requires an accurate determination of the clay studied in terms of its chemistry and phase composition. Some results from previous works do not allow the use of the data for comparison due to uncertainties in the sample purification and characterization (Weaver and Beck, 1971).
- Some pitfalls can also make the interpretation of this method in determining the clay solubility more challenging. Congruent dissolution of clay (Bauer and Berger, 1998; Hofmann et al., 2004; Sato et al., 2003) has been reported as a critical mechanisms for the ability of a system to reach a steady state over time. In fact, nonstoichiometric dissolution do not prevent achieving an equilibrium state as long as the whole chemical system remains correct concerning the Gibbs phase rule (Xie and Walther, 1992).
- Kinetic issues are also key factors in reaching a steady state considering that the dissolution rate is dependent on several physico-chemical parameters (temperature, ionic strength, stirring) and may lead to equilibration duration out of the experiment range.

The aim of this paper is to determine the thermodynamic properties for some well characterized clays, from which chemical composition and impurity information were accurately defined, (Gailhanou et al., 2013; Gailhanou et al., 2009; Gailhanou et al., 2007) from solubility measurements performed at 25 and 40°C and to compare these results with values obtained from calorimetric measurements (Blanc et al., 2014a; Gailhanou et al., 2013; Gailhanou et al., 2007). This allows verification of the equilibrium constants calculated from calorimetric measurements with a different and independent method. In addition, it helps in assessing the thermodynamic database used for calculating the equilibrium constants since the speciation of the solution will be modeled from the ThermoChimie database (Giffaut et al., 2014). This analysis is important because thermodynamic properties measured by calorimetry are to be used in order to simulate equilibrium in aqueous media.

Eventually, to discuss the stability of clay minerals in contact with a solution we are referring to the mass action law, providing to this equation the full list of dissolved element, issued

from chemical analyses. For complex compositions, a geochemical code has been used to avoid approximations in addressing activities from concentrations and activities were assigned with stoichiometric coefficients corresponding to the composition of the natural minerals. The comparison is held with equilibrium constants obtained experimentally with an independent method, using calorimetry measurements.

2. Materials and Method

2.1 Clay minerals selection and characterization

Four clay minerals of interest were studied in the present works including Illite IM-t2, smectite MX80, Santa Olalla vermiculite and chlorite Cca-2. The origin of the clay is reported in Table 1. Kaolinite (Kga-2, source clay) was also studied as a simple system and serves as a control for the following experiments. The SiO_2-Al_2O_3-H_2O system is the most reported in the literature (Devidal et al., 1996; Kittrick, 1966; May et al., 1986) and the most constrained due to its low oxide components.

Table 1 – Origin of the studied clay minerals

Mineral name	Origin	Supplier	Citation
Smectite MX-80	Wyoming, USA	ANDRA	(Gailhanou et al., 2007)
Illite IMt-2	Silver Hill, Montana, USA	Source Clay Project	
Chlorite Cca-2	Flagstaff Hill, California, USA	Source Clay Project	(Gailhanou et al., 2009)
Vermiculite Santa Olalla (SO)	Phalabora, Transvaal, South Africa	Ward's Natural Science	(Gailhanou et al., 2013)

The clay minerals selected for this experimental program are well-representative of clay mineral groups (1:1, 2:1, and 2:1:1). Moreover, they are of great interest considering that they represent the main clay phases constitutive of clay-rock formation.
All these clays were characterized and purified in previous studies (Gailhanou et al., 2013; Gailhanou et al., 2009; Gailhanou et al., 2007) for the determination of thermodynamic properties through calorimetric experiments. Samples were then characterized using chemical analyses (X-ray fluorescence, infrared spectroscopy, ^{57}Fe Mössbauer spectroscopy, CEC, ^{27}Al NMR). Impurities and clay phases were detected and quantified using XRD analyses on oriented powder samples. Chemical analyses were also performed at scales from a few micrometers to a few nanometers by microprobe and TEM-EDX analyses.

The impurity contents and the stoichiometric composition with respect to the dehydrated samples are given in Table 2. The mean structural formulae of the corresponding clay minerals were finally obtained by subtracting the low residual impurities content from the global chemical composition of the samples. In the following work, these structural formulae are used for calorimetric measurements and the *IAP* calculations.

Table 2 – Impurity contents and mean structural formulae of the studied clay systems

Clay	Structural formula	Impurity contents

Kaolinite KGa-2[(1)]	$Si_2Al_{1.98}Fe_{0.02}O_5(OH)_4$	Anatase: 1% Crandallite+mica and/or illite: 1%
Illite IMt-2[(2)]	$K_{0.762}Na_{0.044}(Si_{3.387}Al_{0.613})(Al_{1.427}Mg_{0.241}Fe^{3+}_{0.292}Fe^{2+}_{0.084})O_{10}(OH)_2$	Quartz: 7.65 wt%, Microcline: 2.04 wt%, Rutile: 0.89 wt%, Kaolinite: 0.31 wt%, Chlorite: traces
Smectite MX80[(3)]	$Na_{0.409}K_{0.024}Ca_{0.009}(Si_{3.738}Al_{0.262})(Al_{1.598}Mg_{0.214}Fe^{3+}_{0.173}Fe^{2+}_{0.035})O_{10}(OH)_2$	Quartz: 8.29 wt%, Cristobalite: 8.29 wt%, Amorphous silica: 5.53 wt%
Vermiculite SO[(4)]	$Ca_{0.445}(Si_{2.778}Al_{1.222})(Al_{0.216}Mg_{2.475}Fe^{3+}_{0.226}Fe^{2+}_{0.028})O_{10}(OH)_2$	Quartz 0.3 wt%, cristobalite 0.2 wt%
Chlorite CCa-2[(5)]	$(Si_{2.633}Al_{1.367})(Al_{1.116}Mg_{2.964}Fe^{3+}_{0.215}Fe^{2+}_{1.712}Ca_{0.011})O_{10}(OH)_8$	Rutile: 0.77 wt%

References: (1) (Chipera and Bish, 2001); (2) and (3) (Gailhanou and Blanc, 2007); (4) (Gailhanou et al., 2013); (5) (Blanc et al., 2014a)

2.2 Experimental setting

Clay mineral dissolution experiments are often conducted over very long periods (> 2 years) so that thermodynamic equilibrium can be reached according to the evolution of the dissolution rate. This reaction period is related to the kinetics of dissolution of clay minerals and the evolution of aqueous concentration over time. Several experimental parameters influence the rate of clay dissolution: pH, temperature, ionic strength, stirring and degree of saturation. By considering these experimental parameters, the experiments were conducted at two different temperatures (25°C and 40°C) and by acidifying the initial solution to pH 5 in order to promote dissolution by perturbing the system in an acidic condition. Batches were assembled by preparing a suspension to homogenize the system, which was divided according the different withdrawal times up to the 7 years duration of experiments. A PTFE vessel fitted with a Nalgene cap equipped with a silicon joint was used to prevent any evaporation of the solution along the experimental time and allow for direct centrifugation for the liquid solid separation. The whole process is presented in Figure 1.

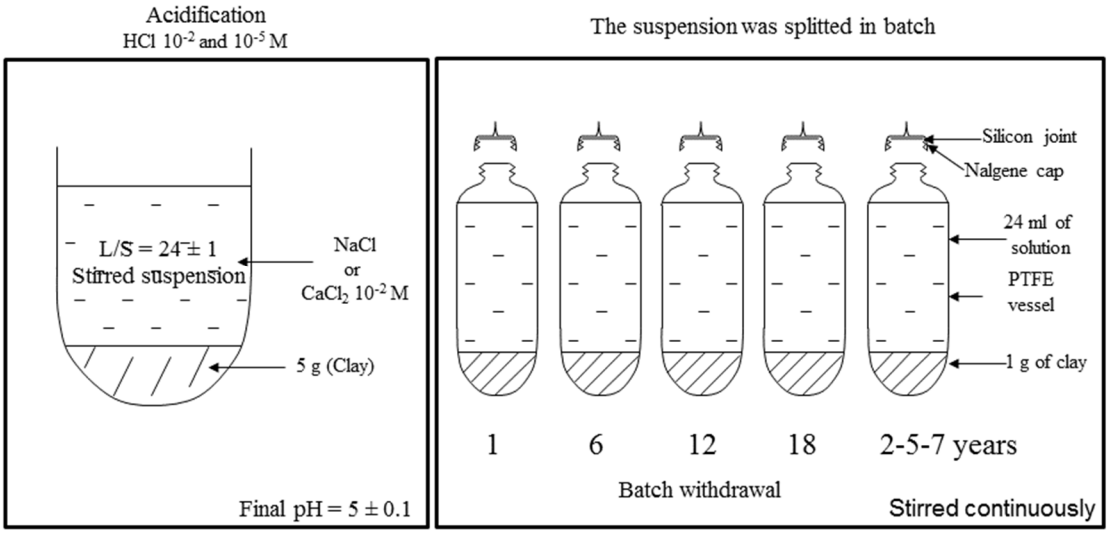

Figure 1 – Scheme representing the protocol used for the equilibration experiments.

For the illite batches, only experiments at 25°C were performed. The available quantity of purified illite samples does not allow performing the experiment at a second temperature (40°C).

The experiments were performed over a period of seven years. For every clay sample, up to six batch experiments were prepared. The suspension of each bottle was sampled after the desired time span. The batches were stored in polypropylene vessels closed with a Nalgene cap equipped with silicon joint to avoid evaporation over the 7 years of experience. They were prepared with a liquid to solid (L/S) ratio of 24 ± 1.

The ionic solution is dependent on the cationic occupation in the specific clay interlayer space. Accordingly, a 10^{-2} M NaCl ionic solution was used for MX80, illite, and kaolinite KGa-2. For Santa Ollala vermiculite and chlorite Cca-2, a 10^{-2} M $CaCl_2$ ionic solution was used. The ionic solution thereby controlled the activity of interlayer cations in solution. For each series of clay, a 24 mL blank (ionic base NaCl or $CaCl_2$) was placed under the same experimental conditions described below. At each withdrawal, a sample was taken and analyzed as a control. The batches were gently stirred continuously during the experiment.

2.3 Solution and analysis

All solutions were prepared with ultra-pure water (Milli-Q 18 MΩ) that was heated to 100°C for 1 h and cooled under a N_2 flux for 2 h prior to its introduction in a N_2 atmosphere glove-box (Jacomex GP, PO2 < 1 ppm) and high grade salts. Solutions were prepared in the glove box by dissolution of analytical grade salts at 25°C.

At each withdrawal, pH, pe and alkalinity of the solutions were determined after centrifugation, and ultrafiltration (10 kD, Millipore Millex-VV, PVDF) in the glove box. Major cations (Na^+, K^+, Ca^{2+}, Mg^{2+}, SiO_2, Al^{3+}, Fe_t) and anions (Cl^-, SO_4^{2-}) were quantified by inductively coupled plasma atomic emission spectrometry (ICP/AES) and ionic chromatography (HPLC, Dionex ICS 3000), respectively. The total volume of the filtered solution (~24 mL) allow us to avoid any dilution before measurement of the aqueous concentration of interest. The electronegativity was assumed for each withdrawal. The remaining solids were freeze-dried and stored at room temperature in order to be characterized.

2.4 Postmortem clay characterization

X-ray diffraction analysis, infra-red (IR) spectroscopy, transmission electron microscopy and cation exchange capacity (CEC) analyses were performed on the solids recovered at the end of the experiments up to 7 years for kaolinite, smectite, vermiculite and chlorite and up to 5 years for illite. These analyses were performed to detect any dissolution of the impurities characterized in the initial purified samples (Table 2) and other possible phases precipitated during the experiment.

3. Thermodynamic calculations

3.1 Theoretical background

Applying the Mass action law allows one to define the ionic activity product (IAP or Q):

$$IAP = Q = \prod_i a_i^{vi} \qquad \text{(Eq. 1)}$$

where a_i and ν_i stand for the activity and the stoichiometric coefficient of the dissolved aqueous species involved in the equilibrium reaction, respectively. In the present case, given the low ionic strengths of the solution, the Debye-Hückel model is used for calculating the activity coefficients of the aqueous complexes. For clay minerals specifically, including their compositional complexity, the IAP product could be simplified as follow:

$$IAP = \{interlayer\ component\}^{n1} \cdot \{tetrahedral\ component\}^{n2}\ \{octahedral\ component\}^{n3}\ \{OH\}^{n4}$$

where n1 to n4 correspond to the number of ions in the structural formula of the considered clay

For a theoretical low-charge montmorillonite of composition $Na_{0.33}(Al_{1.67}Mg_{0.33})Si_4O_{10}(OH)_2$, the IAP product corresponds to:

$$IAP = \frac{\left(a_{H_4SiO_4}\right)^4 \cdot \left(a_{Mg^{2+}}\right)^{0.33} \cdot \left(a_{Al^{3+}}\right)^{1.67} \left(a_{Na^+}\right)^{0.33}}{\left(a_{H_2O}\right)^4 \cdot \left(a_{H^+}\right)^6} \quad \text{(Eq. 2)}$$

From this expression, it appears that the exchange reaction between the interlayer (Na^+ in this case) and the cations in solution may affect the IAP. One way to limit this displacement is to perform the equilibration in an aqueous media whose main electrolyte corresponds to the interlayer cation.

Considering the equilibrium reaction for a theoretical solid AB ($AB \overset{K_{AB,P,T}}{\longleftrightarrow} A^+ + B^-$), the mass action law states that at equilibrium:

$$K_{AB,T,P} = \frac{\prod_i a_i^{\nu i}}{a_{AB}} \text{ since } a_{AB} = 1, \text{ then } K_{AB,T,P} = \prod_i a_i^{\nu i} = Q_{AB} \quad \text{(Eq. 3)}$$

Reaching equilibrium is a common issue for clay minerals in contact with aqueous solutions. It is then necessary to define the degree of supersaturation (or undersaturation) of a solid with respect to an aqueous solution. Supersaturation occurs when $Q_{AB,P,T}$ is higher than $K_{AB,P,T}$ whereas undersaturation implies that $Q_{AB,P,T}$ is lower than $K_{AB,P,T}$.

The assessment of thermodynamic equilibrium also depends on the phase rule:

$$F = (2) + C - P \quad \text{(Eq. 4)}$$

where F is the reaction's degree of freedom, C is the number of independent chemical components and P is the number of phases in the system. At constant pressure and temperature, it follows that the maximum number of phases at equilibrium corresponds to the number of independent components except H_2O. For kaolinite equilibrium in pure water, at constant pressure and temperature and in the SiO_2-Al_2O_3-H_2O chemical system, applying relation (4) gives two degrees of freedom, meaning that a maximum of two phases can be at equilibrium simultaneously, in agreement with the predominance diagram (Figure 2). If more than 2 phases are observed in the final products (kaolinite + amorphous silica + gibbsite, for instance), the assemblage would be considered in metastable equilibrium and equilibrium constant could not be extracted from the concentrations in solution.

For the other clay minerals, the situation is similar but the number of degrees of freedom is higher because their composition is more complex. The electrolyte media (NaCl) provides 1 additionnal degree of freedom, while Cl is not included in the budget because it cannot be precipitated as a mineral in our systems. Ti is also not considered in these calculations.

Applying the Gibbs Phase Rule provides 6 degrees of freedom for smectite MX-80, illite IMt-2, Vermiculite SO and 5 for chlorite Cca-2.

Equilibrium with a secondary phase, other than the main phase, may modify concentrations of dissolved elements, as reported by May et al. (1986) for the control of aluminium by gibbsite when equilibrating smectite in solution. However, according to the Gibbs phase rule, just the equilibrium with gibbsite does not prevent smectite to reach equilibrium.

3.2 Congruent Dissolution

In the SiO_2 –Al_2O_3 – H_2O system, the IAP product can be written in a simplified manner as follows by considering a congruent or a noncongruent dissolution:

$$IAP = = \frac{\{Al^{3+}\}\cdot\{H_4SiO_4\}}{\{H^+\}^3} \quad \text{congruent}$$

$$IAP = = \frac{\{Al^{3+}\}}{\{H^+\}^3} \cdot LogK_{am.SiO_2} \quad \text{non congruent} \qquad \text{(Eq. 5)}$$

The IAP is thus dependent of the activity of each structural component of the clay mineral. If we consider the SiO_2-Al_2O_3-H_2O system, the activity of the interlayer cations is nil. The system is simplified by considering the activity of the tetrahedral and octahedral cations and the protonation/deprotonation related to the surface charge of clays as a function of the dissolution/reprecipitation processes (Xie and Walther, 1992). Figure 2 shows the different reaction pathways for reaching equilibrium with kaolinite. This illustration thus shows that every reaction pathways, congruent (pathway 1) and noncongruent (pathways 2 and 3), end in equilibrium with kaolinite. When the activity of dissolved SiO_2 is controlled by a phase (amorphous silica, pathway 3), the equilibrium will be reached by modifying the activity of dissolved Al_2O_3 or the activity of the proton in solution, consistent with the Gibbs phase rule in which both kaolinite and amorphous SiO_2 are at equilibrium. It is obvious that the congruent pathway crosses over the gibbsite domain meaning that either gibbsite was metastable and did not precipitate or was at thermodynamic equilibrium and thus the congruent dissolution did not occur and is purely theoretical.

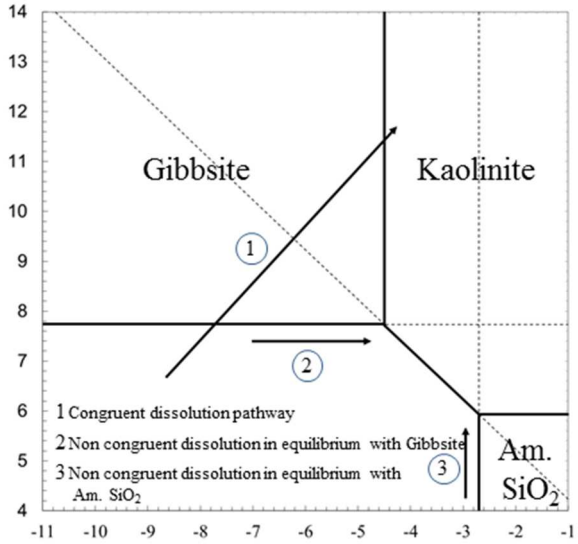

Figure 2 – Activity diagram of $\{Al^{3+}\}/\{H^+\}$ versus $\{H_4SiO_4\}$ in the SiO_2-Al_2O_3-H_2O system

3.1 IAP formulation and calculation tools

The law of mass action depends on the precise stoichiometric composition for the mineral studied and on the activity of the aqueous species used in the dissolution equation in agreement with the thermodynamic database used. Accordingly, for the clay minerals studied, the dissolution equation and the associated expression of the ionic activity product are given in Table 3. *IAP*, saturation indexes and predominance diagrams were calculated from the chemical compositions of the solution using PHREEQC (Parkhurst, 1995) and Phreeplot (Kinniburgh and Cooper, 2011) coupled with the ThermoChimie database (Giffaut et al., 2014). The latter is consistent with Thermoddem (Blanc et al., 2012) for the calculations performed here. Consistent with the low ionic strength of the experimental solutions, activity coefficients of the charged species were calculated using the extended Debye-Hückel equation. The standard state adopted in this study for the solid phases and H_2O is unit at the pressure and temperature of interest for the pure minerals and fluid.

Because the distribution of each ion of Al, Fe, Mg, Ca, Na or K in aqueous solution depends on pH and the total analytical concentration of the ions, we used a geochemical code (PhreeqC) to address the relative amount of aqueous species and their activities, based on measured concentrations. Once activities of each type are obtained, IAP are calculated, for each mineral, considering equations reported in Table 3.

Table 3 – Equilibrium reactions for the minerals considered and the associated IAP.

Clay	Reaction	Al/Si	Mg/Si
Kaolinite KGa-2	$Al_{1.98}Si_2Fe_{0.02}O_{4.995}(OH)_4 + 5.99H^+ \leftrightarrow 1.98Al^{3+} + 2H_4SiO_4 + 0.01Fe^{2+} + 0.01Fe^{3+} + 0.995H_2O$ $IAP = \{H_4SiO_4\}^2 \cdot \{Al^{3+}\}^{1.98} \cdot \{Fe^{2+}\}^{0.01} \cdot \{H^+\}^{-5.99}$	0.99	/
Illite IMt-2	$(Na_{0.044}K_{0.762})(Si_{3.387}Al_{0.613})(Al_{1.427}Fe_{0.376}Mg_{0.241})O_{10}(OH)_2 + 8.452H^+ + 1.548H_2O \leftrightarrow 2.04Al^{3+} + 3.387H_4SiO_4 + 0.084Fe^{2+} + 0.292Fe^{3+} + 0.241Mg^{2+} + 0.044Na^+ + 0.762K^+$ $IAP = \{Na^+\}^{0.044} \cdot \{K^+\}^{0.762} \cdot \{H_4SiO_4\}^{3.387} \cdot \{Al^{3+}\}^{2.04} \cdot \{Fe^{2+}\}^{0.084} \cdot \{Fe^{3+}\}^{0.292} \cdot \{Mg^{2+}\}^{0.241} \cdot \{H^+\}^{-8.452}$	0.6	0.07
Smectite MX-80	$Na_{0.409}K_{0.024}Ca_{0.009}(Si_{3.738}Al_{0.262})(Al_{1.598}Mg_{0.214}Fe_{0.208})O_{10}(OH)_2{:}5.189H_2O + 7.048H^+ \leftrightarrow 1.86Al^{3+} + 3.738H_4SiO_4 + 0.035Fe^{2+} + 0.173Fe^{3+} + 0.214Mg^{2+} + 0.409Na^+ + 0.024K^+ + 0.009Ca^{2+} + 2.237H_2O$ $IAP = \{Na^+\}^{0.409} \cdot \{K^+\}^{0.024} \cdot \{Ca^{2+}\}^{0.009} \cdot \{H_4SiO_4\}^{3.738} \cdot \{Al^{3+}\}^{1.86} \cdot \{Fe^{2+}\}^{0.035} \cdot \{Fe^{3+}\}^{0.173} \cdot \{Mg^{2+}\}^{0.214} \cdot \{H^+\}^{-7.048}$	0.49	0.06
Vermiculite SO	$Ca_{0.445}(Si_{2.778}Al_{1.222})(Al_{0.216}Mg_{2.475}Fe_{0.254})O_{10}(OH)_2 + 10.888H^+ \leftrightarrow 1.438Al^{3+} + 2.778H_4SiO_4 + 0.028Fe^{2+} + 0.226Fe^{3+} + 2.475Mg^{2+} + 0.445Ca^{2+} + 0.888H_2O$ $IAP = \{Ca^{2+}\}^{0.445} \cdot \{H_4SiO_4\}^{2.778} \cdot \{Al^{3+}\}^{1.438} \cdot \{Fe^{2+}\}^{0.028} \cdot \{Fe^{3+}\}^{0.226} \cdot \{Mg^{2+}\}^{2.475} \cdot \{H^+\}^{-10.888}$	0.51	0.89
Chlorite Cca-2	$(Mg_{2.964}Fe_{1.927}Al_{1.116}Ca_{0.011})(Si_{2.633}Al_{1.367})O_{10}(OH)_8 + 17.468H^+ \leftrightarrow 2.483Al^{3+} + 2.633H_4SiO_4 + 1.712Fe^{2+} + 0.215Fe^{3+} + 2.964Mg^{2+} + 0.011Ca^{2+} + 7.468H_sO$ $IAP = \{H_4SiO_4\}^{2.633} \cdot \{Al^{3+}\}^{2.483} \cdot \{Fe^{2+}\}^{1.712} \cdot \{Fe^{3+}\}^{0.215} \cdot \{Mg^{2+}\}^{2.964} \cdot \{H^+\}^{-17.468}$	0.94	1.1

3.2 Uncertainty calculation

The uncertainty for the *IAP* was calculated from the analytical uncertainty in the different parameters quantified (pH, anions, cations). The measurement uncertainty was defined as a parameter associated with a measurement, which characterizes the dispersion of values that

could reasonably be attributed to the person who took the measurements (Danzer, 2007). In general, the measurement uncertainty value comprises several components. The value measured and any relationship that exists between it and parameters p_1, p_2, and p_3, which are the activities of elements on which it depends, must be reviewed. This can be done by establishing a mathematical equation, y = f (p_1, p_2, p_3, etc.). The calculation starts with estimating the size of each uncertainty for each parameter (pH, aqueous concentrations). We ignore the insignificant values because the calculation for uncertainty propagation is based on the sum of squares. The significant values are then introduced in the form of standard deviation $u(p_i)$. In cases where the parameters are independent of each other, the calculation for uncertainty propagation is given according to the following equation:

$$u\big(y(p_1, p_2, \ldots)\big) = \sqrt{\left(\frac{\delta y}{\delta p_1}\right)^2 \cdot \big(u(p_1)\big)^2 + \left(\frac{\delta y}{\delta p_2}\right)^2 \cdot \big(u(p_2)\big)^2 + \cdots} \qquad \text{(Eq. 6)}$$

4. Results

4.1 Kaolinite KGa-2

All the aqueous concentrations measurements over the 7 years period were reported in Table 4, as the calculated IAP. During this time, after the first withdrawal, the experiments exhibited a steady state of Si and Al concentrations and decreasing pH. The Si content reaches a stationary state at Si concentrations close to amorphous silica solubility (Table 1S).

Table 4 – Aqueous solutions equilibrated with kaolinite KGa-2 up to 7 years and the calculated log IAP

Time (day)	Ionic strength	T°C	pH	pe	Na	K	Fe	Si	Al	*Log IAP*	Al/Si
					µmol.kg^{-1}						
1	0.01	23.8	5.0	5.12	9770	161.1	0.370	103	1.39	9.31	0.01
182	0.01	24.5	4.8	8.57	10091	207.2	0.060	471	1.20	9.34	0.002
365	0.01	24.8	4.8	8.00	10574	94.6	0.056	501	1.06	9.41	0.002
547	0.01	22.8	4.5	9.00	10200	143.0	0.077	667	1.42	8.07	0.002
730	0.01	22.3	4.5	9.59	10509	127.9	0.013	721	1.17	7.76	0.001
2500	0.01	24.6	4.2	8.00	10983	181	0.11	1048	1.00	6.54	0.001
1	0.01	35.4	4.9	6.46	12018	281.3	0.057	213	1.13	8.84	0.005
182	0.01	39.4	4.7	7.91	12419	327.4	0.060	797	1.58	9.06	0.002
365	0.01	38.3	4.7	6.60	12440	225.1	0.095	672	1.19	8.66	0.001
547	0.01	39.6	4.4	7.05	11300	322.0	0.045	801	1.80	7.32	0.002
730	0.01	39.6	4.2	8.91	13249	370.9	0.048	979	3.06	6.80	0.003

According to the SiO_2-Al_2O_3-H_2O stability diagram (Figure 3), the decrease in $\{Al^{3+}\}/\{H^+\}^3$ ratio results from the pH decrease and not from a decrease in aluminum concentration. Equilibrium appears to have been reached from oversaturation, at least at 25°C over the seven years of interaction, given to the uncertainties. The dissolution of kaolinite is nonstoichiometric with a preferential release of silicon. Wieland and Stumm (1992) demonstrated that during the kaolinite dissolution process, the dissolved aluminum in solution is simultaneously readsorbed on the surface of the kaolinite causing the experimentally observed nonstoichiometry and leading to proton mediated dissolution.

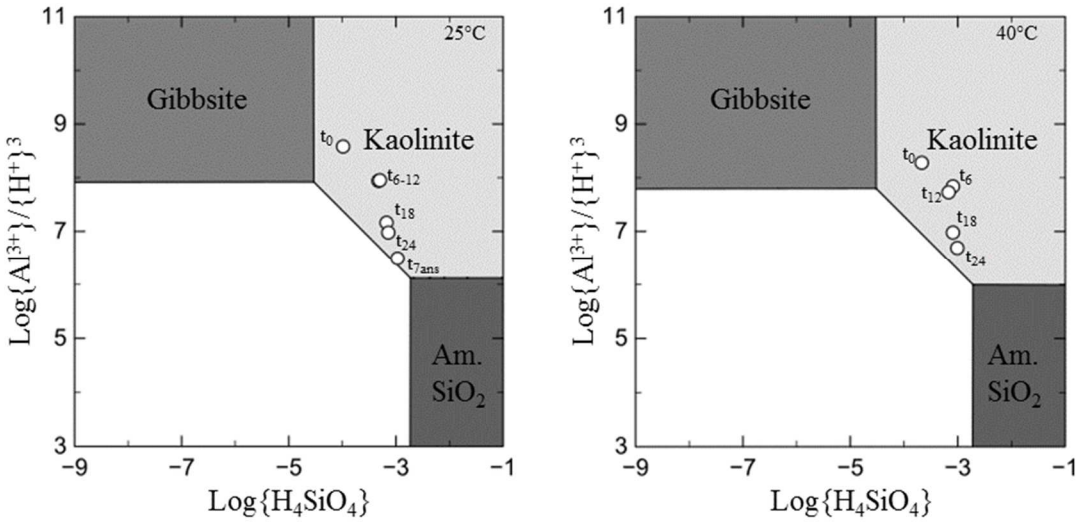

Figure 3 – Composition of solutions equilibrated with kaolinite KGa-2 in the SiO_2-Al_2O_3-H_2O stability diagram at 25°C, 1 bar. The white circles represent the solution compositions analyzed over 7 years for the system at 25°C and 40 °C.

As for the Gibbs phase rule, the SiO_2-Al_2O_3-H_2O subsystem provides 2 degrees of freedom, which number is not decreased because neither amorphous silica, nor Gibbsite reach equilibria in our experiments. Equilibrium with kaolinite is thus consistent with the Gibbs phase rule in our system.

4.2 Illite IMt-2

All the concentrations of elements considered in the calculation of the IAP were displayed in the Table 5. As aforementioned, the final point of this aqueous equilibrium system occurs after 5 years experiment timeframe. Over this elapsed time, the concentrations of silica and potassium in solution, displayed in Table 5, increased up to the first year and then dropped until the end of the experiment. For silica, the decrease that was deferred is slow, reaching an apparent steady state. For the other considered elements (Fe, Mg, Al), the concentrations showed a general decrease over time. From the beginning of the experiment the pH reaches a steady state over 6, increasing to 7.8 at the last withdrawal.

Table 5 – Aqueous solutions equilibrated with Illite IMt-2 up to 5 years and the calculated log IAP

Time (day)	Ionic strength	T°C	pH	pe	Na	K	Fe	Mg	Si	Al	*Log IAP*
					µmol.kg^{-1}						
3	0.01	25	6.6	8.3	10006	505.3	14.21	8.23	176.11	0.127	12.95
60	0.01	25	5.9	8.5	10006	586.3	2.31	7.96	316.19	0.527	13.58
365	0.01	25	6.5	8.5	10006	573.3	2.18	4.11	315.19	0.600	14.70
730	0.01	25	6.4	8.6	10006	344.2	0.71	2.83	141.08	0.297	12.48
1825	0.01	25	7.8	9.0	12108	164.1	0.25	3.50	93.26	0.322	11.42

The saturation indexes (Figure 4) calculated from the above concentrations allow visualizing the steady state of silica concentration and could be explained by the presence of quartz which is the main impurity detected in the characterization of the illite IMt-2. The evolution of Si, Al and K activity with an increase followed by a decrease over the last 4 years of the experiment

could be related to precipitation of K bearing phases as displayed in the Figure 4. Both quartz and microcline were identified in the purified sample before the experiments. According to the Gibbs phase rule, no more than 7 phases could precipitate in the NaO-K_2O-SiO_2-Al_2O_3-MgO-FeO-Fe_2O_3-H_2O system. Considering the calculated saturation indexes, quartz, K-feldspar, albite and gibbsite are close to equilibrium. In addition, kaolinite and chlorite have been identified as potential impurities. Supposing that, in the worst case, all those minerals are reaching equilibrium leaves 1 degree of freedom for illite equilibrium, which is thus consistent with the Gibbs phase rule.

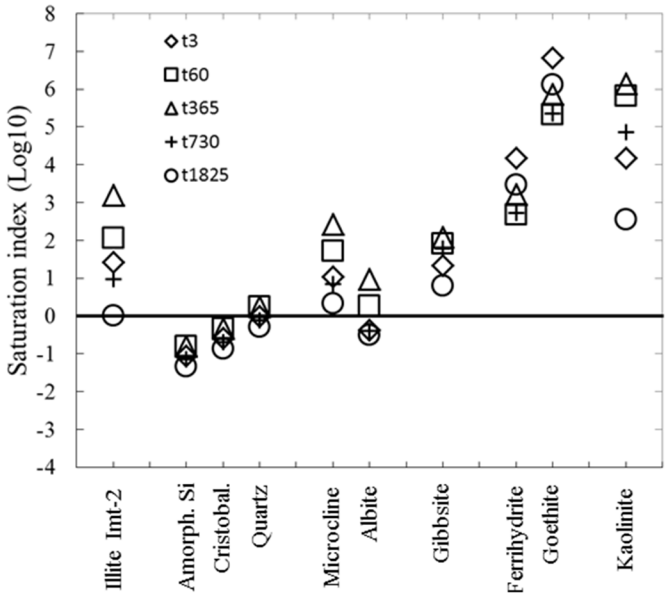

Figure 4 - Saturation indexes with respect to solutions equilibrated with Illite IMt-2 at 25°C

4.3 Smectite (MX80)

The variations of pH and Na, K, Ca, Fe, Mg, Si, and Al concentrations with time are shown in Table 6.

Table 6 – Aqueous solutions equilibrated with Smectite MX-80 up to 7 years and the calculated log IAP

Time (day)	Ionic strenght	T°C	pH	pe	Na	K	Ca	Fe	Mg	Si	Al	log IAP
					µmol.kg-1							
1	0.01	22.4	5.3	4.0	14224	204.6	48.20	0.17	3.68	427.7	0.16	6.27
182	0.02	24.4	4.9	7.2	15050	28.1	8.00	0.18	3.70	1116.6	0.64	6.50
365	0.02	25.4	4.9	7.5	15307	30.7	7.00	0.02	3.70	1043.4	0.57	5.95
547	0.01	22.8	4.9	9.0	14700	43.5	6.84	0.01	3.70	1240.0	0.30	5.96
730	0.02	24.1	5.0	8.9	15281	40.9	2.79	0.05	3.17	1214.8	0.10	5.11
2500	0.01	24.6	5.0	8.9	10835	48.61	> D.L.	0.05	1.73	773.9	0.23	5.39
1	0.01	39.1	5.5	6.5	15711	92.1	9.66	0.05	5.19	712.2	0.53	7.17
182	0.02	40.1	5.0	6.8	16107	104.9	8.50	0.11	5.00	1273.1	0.29	5.58
365	0.02	37.0	5.0	7.0	16947	38.4	8.50	0.17	5.00	1239.8	0.19	5.38
547	0.02	38.8	4.7	7.3	16800	68.3	8.53	0.18	5.72	1530.0	0.21	4.19
730	0.02	39.6	4.6	8.2	17221	30.7	7.88	10.40	5.80	1402.9	0.17	3.83

Release of Ca, K, and Si underwent a distinct transition from the initial withdrawal of rapid release to significantly lower release the following time. Al concentrations increase over the first year and gradually decrease until the end of the experiment. High initial cation (Ca, K) release rates reflect rapid selective leaching of the exchangeable cation for sodium, the latter being the element constituting the ionic solution (NaCl, 10^{-2} M) used in this set of experiments. The rapid release of Si could be explained by dissolution of amorphous silica as previously demonstrated by (Metz et al., 2005). Quartz and amorphous silica were both detected in the initial sample used for the aqueous equilibrium. The behavior of dissolved Al could be related to precipitation of aluminous phases. This assumption could be verified by calculating the saturation indexes with respect to the dissolved ions in solution. In the Na_2O-K_2O-CaO-SiO_2-Al_2O_3-Fe_2O_3-FeO-MgO-H_2O system, we observe that several elements could be controlled by phases (Figure 1S). Silicon, aluminum, trivalent iron and potassium could be controlled by several phases (Figure 1S) such as amorphous silica and/or cristobalite, gibbsite, and ferrihydrite, respectively. Increased proton activity in solution was more marked at 40°C.

Activity diagrams displayed in Figure 5 indicates that equilibrium could be reached for smectite MX-80, especially when the energetic contribution of interlayer cation solvation is considered, providing an increase of the smectite stability domain.

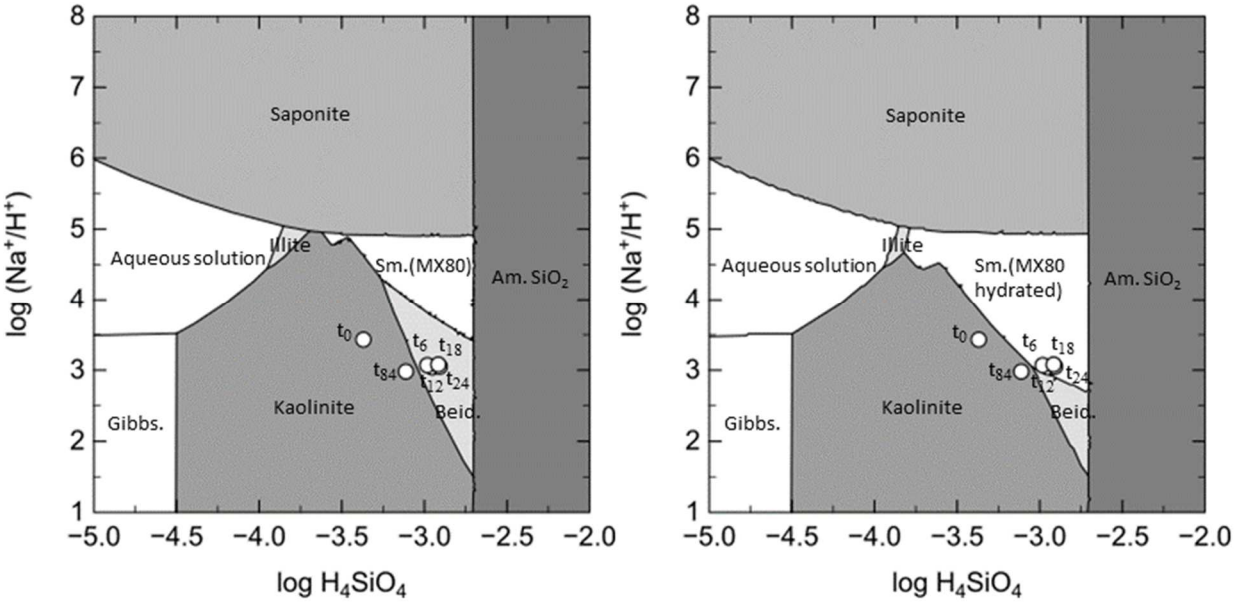

Figure 5 – Stability diagram of log {Na^+}/{H^+} versus log {H_4SiO_4} activity illustrating the solubility of clays in the SiO_2-Na_2O-H_2O system. The stability diagrams were calculated according to the water energy contribution of smectite MX-80 from an anhydrous to an hydrated states. The white circles represent the aqueous solution compositions of the solutions analyzed for the 7 years of experiments for the system at 25 °C. The abbreviations are defined as follows: Am. SiO_2., Sm., Gibbs., Beid. for amorphous SiO_2 solution, smectite, gibbsite, and beidellite, respectively.

In applying the Gibbs phase rule to the Na_2O-K_2O-CaO-SiO_2-Al_2O_3-Fe_2O_3-FeO-MgO-H_2O system we can consider the possible equilibrium with amorphous silica, gibbsite and ferrihydrite (Figure 1S). Possible impurities corresponds to silica polymorphs, which does not remove additional degrees of freedom and then 8 – 3 = 5 degrees remain, consistent with smectite equilibrium in this experiment.

4.4 **Vermiculite (SO)**

The aqueous solutions equilibrated with vermiculite SO and the associated IAP were given in Table 7. The concentrations of the considered elements in the calculation, pH, and pe of the IAP were displayed for each withdrawal at both 25 and 40°C and above for the 7 years duration of the experiments. The solutions were undersaturated with respect to vermiculite. According to the Mg/Si ratio in aqueous solution, the vermiculite seems initially to dissolve congruently (after 1 day). Then, the release of Si and Al underwent a distinct transition from the initial withdrawal of rapid release to a significantly lower release the next time. For K, Ca, and Fe concentrations, a steady state is observed over the time experimented; only Mg shows a slight increase after the second withdrawal. No evolution of the CEC was observed on the solid recovered at the end of the experiment with values of 1.76 ± 2 and 1.72 ± 2 $mmol.g^{-1}$ for the first and last withdrawals, respectively. Nonetheless the fraction of exchangeable cations evolved over the 7 years of experiment. At initial state the distribution of exchangeable cation was 96 and 4 % of Ca and Mg while after 7 years the distribution was 88 and 11 % of Ca and Mg, respectively, displaying an adsorption of magnesium. The main evolution was from the proton activity, which was reduced from -5 to -7 and -7.5 at 25 and 40°C, respectively.

Table 7 – Aqueous solutions equilibrated with Vermiculite SO up to 7 years and calculated IAP

Time (day)	Ionic strength	T°C	pH	pe	K	Ca	Fe	Mg	Si	Al	*IAP*	*Mg/Si*
					$\mu mol.kg^{-1}$							
1	0.05	23.3	5.2	5.3	302	14951	0.412	1880	1494	41.065	29.44	1.25
182	0.05	24.0	6.5	6.8	384	14624	0.027	2444	751	0.585	36.33	3.25
365	0.05	24.1	6.6	7.2	266	15083	0.072	2715	679	0.204	36.22	3.99
547	0.05	22.5	6.8	7.2	284	14800	0.035	2670	691	0.191	37.61	3.86
730	0.05	23.8	6.9	7.0	300	14700	0.006	2500	700	0.070	37.11	3.57
2500	0.03	24.6	7.3	7.0	296	8483	>0.002	977.5	585.9	0.1	37.99	1.67
1	0.05	35.7	5.2	5.3	583	14636	0.026	1847	1609	16.752	27.86	1.14
182	0.06	39.6	6.6	7.3	685	16238	0.200	2267	870	0.332	34.31	2.60
365	0.06	36.5	6.7	5.2	573	16915	0.139	2510	749	0.272	35.08	3.35
547	0.06	39.9	7.5	5.9	632	16800	0.446	2600	792	0.206	38.56	3.28
730	0.06	39.7	7.5	6.1	700	16600	0.080	2400	800	0.080	38.07	3

In the $CaO\text{-}FeO\text{-}Fe_2O_3\text{-}MgO\text{-}SiO_2\text{-}Al_2O_3\text{-}H_2O$ system, saturation indexes were calculated according to the aqueous concentrations experimental time period (Table 2S). It is obvious that proton activity is the main variable affecting the variation of the IAP in the evolution of the IAP over the 7 years of experiments (Figure 6).

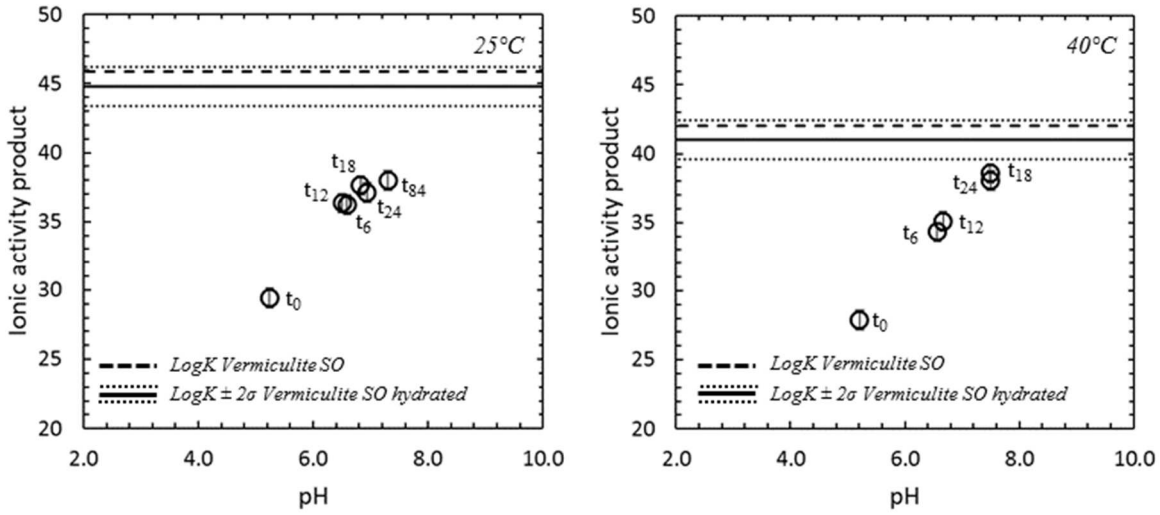

Figure 6 – Comparison of the vermiculite SO IAP values with equilibrium constants calculated from thermodynamic properties measured from Gailhanou et al. (2013) (dotted and black lines) at 25°C and 40°C.

Applying the Gibbs phase rule to the K_2O-CaO-SiO_2-Al_2O_3-Fe_2O_3-FeO-MgO-H_2O system we can consider the possible equilibrium with amorphous silica, gibbsite and ferrihydrite (Figure 2S). Possible impurities corresponds to silica polymorphs, which removes 1 additional degree of freedom and then 7 – 2 = 5 degrees remain, consistent with vermiculite equilibrium in this experiment.

4.5 Chlorite Cca-2

The ionic activity products according to the equilibrium reactions (Table 2) and according to the mass action law are presented in (Figure 7). For the chlorite experiment, the solution was undersaturated with respect to ripidolite Cca-2. At 25 and 40°C, the saturation index was -8.3 and -9.6 log units, respectively, up to the 7 and 2 years of interaction.

Table 8 – Aqueous solutions equilibrated with Chlorite Cca-2 up to 7 years

Time (day)	Ionic strenght	T°C	pH	pe	K	Ca	Fe	Mg	Si	Al	IAP	Mg/Si
					µmol.kg^{-1}							
1	0.03	24.0	5.3	4.8	1054	8117	14.325	757	374	2.539	45.06	2.02
182	0.03	24.9	5.7	6.9	1207	8673	0.598	979	925	0.215	47.01	1.05
365	0.03	24.2	5.9	7.3	1021	8848	0.104	1111	962	0.117	47.47	1.15
547	0.03	23.1	6.2	8.1	1090	8660	0.063	1090	1130	0.056	48.21	0.96
730	0.03	25.0	6.2	7.7	1123	9082	0.032	1057	1172	0.953	50.75	0.90
2500	0.03	24.6	6.2	7	225	8358	17.91	253	1240	0.1	52.97	0.20
1	0.03	38.2	5.1	5.7	1673	10148	4.300	983	1003	1.549	41.97	0.98
182	0.04	38.8	5.6	5.8	1872	10233	0.797	1329	1875	0.221	45.04	0.70
365	0.04	37.3	5.7	6.0	1596	10846	0.129	1510	1686	0.305	46.20	0.89
547	0.04	40.6	5.8	6.3	2070	10900	0.181	1530	1900	0.295	46.16	0.80
730	0.04	39.6	6.1	5.0	1811	11428	0.034	1535	1766	0.050	46.49	0.86

The experiments exhibit no evolution of the aqueous concentration after the first withdrawal (Table 8). A dissolution plateau is characterized for each element constitutive of the multi-

oxides chlorite composition. The average Mg/Si ratio in aqueous solution is in good agreement with the molar ratio in the mineral indicating stoichiometric dissolution of chlorite. pH increases at both temperatures over the 2 years of experiments by 1 unit. At 25°C, after 7 year of interaction, concentrations of iron, potassium and magnesium in solution display opposite evolutions. The two latter concentrations dropped while the concentration of iron increases. Saturation indexes calculation (Figure 3S) indicate a steady state with respect to mineral phases, as gibbsite and amorphous silica at both 25°C and 40°C. Over the 2 years of experiments, Fe^{3+} and Fe^{2+} phases seems to be in equilibrium with the solutions while after 7 years, the solution are oversaturated with respect to iron phases.

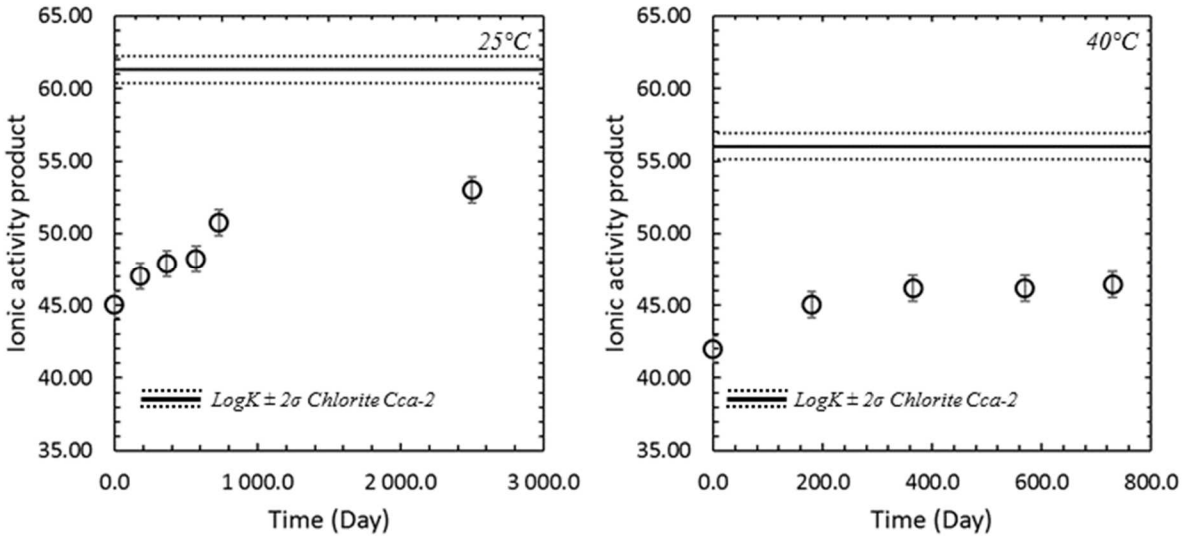

Figure 7 – Comparison of chlorite CCa-2 IAP values with equilibrium constants calculated using thermodynamic properties measured from Gailhanou et al. (2013) (gray areas) at 25°C and 40°C.

The Gibbs phase rule states that in the $CaO\text{-}SiO_2\text{-}Al_2O_3\text{-}MgO\text{-}Fe_2O_3\text{-}FeO\text{-}H_2O$ experimental system, six mineral phases can be at equilibrium at the same time. We observed that according to Figure 3S, silicon and aluminium activities could be potentially controlled by amorphous silica and Gibbsite. No impurities other than rutile was reported from Table 2, which leaves 7 – 2 = 5 degrees of freedom, consistent with chlorite equilibria in this experiment.

5. Discussion

5.1 Clay dissolution experiments

Five clay samples were studied through aqueous equilibrium experiments. The clays in this study were previously analyzed by calorimetry (Blanc et al., 2014b; Gailhanou et al., 2013; Gailhanou et al., 2007) to extract their thermodynamic properties. The equilibrium constants calculated from the calorimetry data are given in Table 9. For both smectite MX-80 and vermiculite, the equilibrium constants are provided in the anhydrous and the hydrated state. For the latter, thermodynamic properties in the anhydrous state are combined with hydration properties extracted by (Gailhanou et al., 2017) and (Vieillard et al., 2019) to provide equilibrium constant for hydrated phases, at 25 and 40°C, as detailed by (Gailhanou et al., 2017). The contribution of the hydration energies is illustrated in Figure 5, where stability diagrams are calculated for both the anhydrous state and the hydrated states. Solvation of

interlayer cation tends to stabilize the montmorillonites and to expand the stability domain, as reported by (Vieillard et al., 2019).

Table 9 – IAP and solubility product calculated from the same set of purified clays

Clay minerals	*IAP**	Solubility product (Calorimetric data)	S.I.	*IAP**	Solubility product (Calorimetric data)	S.I.
	25°C			40°C		
Kaolinite KGa-2	6.61 ± 0.7	6.46 ± 0.6 (1)	0.2	6.8 ± 0.7	5.06 ± 0.6	1.7
Illite IMt-2	11.42 ± 0.7	11.52 ± 1.6 (2)	-0.1		9.59 ± 1.6 (2)	
Smectite (MX80)	5.39 ± 1.7	5.26 ± 1.7 (2)	0.1	3.83 ± 1.7	3.72 ± 1.4	0.1
Smectite (MX80) hydrated	5.39 ± 1.7	4.80 ± 1.7 (3)	0.6	3.83 ± 1.7	3.33 ± 1.7	0.5
Vermiculite (SO)	37.99 ± 0.7	45.89 ± 1.4 (4)	-7.9	38.07 ± 0.7	42.00 ± 1.4	-3.3
Vermiculite (SO) hydrated	37.99 ± 0.7	44.77 ± 1.4 (5)	-6.8	38.07 ± 0.7	41.01 ± 1.4	-2.9
Chlorite CCa-2	52.97 ± 0.9	61.31 ± 1.3 (6)	-8.3	46.49 ± 0.9	56.01 ± 1.3	-9.51

*This work; (1)-modified from (Blanc et al., 2012); (2) (Gailhanou et al., 2007); (3); (4) (Gailhanou et al., 2013); (5); (6) (Gailhanou et al., 2009)

In all the analyzed solutions, displayed in Tables 4 to 8, pH evolves with time. This pH dependence could be linked to the adsorption of H^+ and OH^- ions onto the mineral surfaces, which are metal cation specific and differ from the constituent oxides components (Carroll-Webb and Walther, 1988; Tournassat et al., 2004; Xie and Walther, 1992). This charge is pH dependent and may originate not within the interior of the layers as with the permanent charge but rather on the basal surfaces of the tetrahedral sheets (in 2:1 clays), on the basal surfaces of both tetrahedral and octahedral sheets (in 1:1 clays), and along the edges of the sheets of both 1:1 and 2:1 clays (Tournassat et al., 2016). This charge results from the hydrolysis of broken Si-OH and Al-OH bonds along the surface of clay lattice. These surface hydroxyls can act as either an acid or a base and can react further with H^+ or OH^-, which could explain the different pH evolution in the experiments. pH was willingly kept unbuffered in our systems since it would favor the establishment of a neutral mineral surface in contact with low ionic strength solution and it would minimize the influence of metal complexation (Kriaa et al., 2009) on calculated IAP values.

From the analyzed solution and using the PhreeqC code, IAP could be calculated. Calculation indicates for kaolinite, illite and smectite initial super saturated solutions whereas for vermiculite and chlorite, the solutions are initially under saturated. In the early stages, the concentrations of the elements in solution could be driven by several processes such as cationic exchange capacity, rapid dissolution of (i) small particles, (ii) highly reactive sites on the mineral surface (Kohler et al., 2005) or (iii) nanocrystalline oxides impurities. Another explanation could reside in differences in dissolution rates, which could be much slower for chlorite and possibly vermiculite, as explained further.

Reaction products had been checked by XRD, as displayed in Figure 8 for Illite, without revealing secondary phases precipitation, for any of the experiments. Amorphous phases could still be obtained without being detected by XRD. Saturation indexes calculations indicates that it could be the case for amorphous silica and ferrihydrite, for both MX-80 smectite and chlorite. Applying the Gibbs phase rule in our system provides a number of degrees of freedom consistent with thermodynamic equilibrium, as reported in the Results section. In that regard, noncongruent dissolution resulting from the precipitation of limited number of secondary phases would not prevent the clay mineral to reach equilibrium.

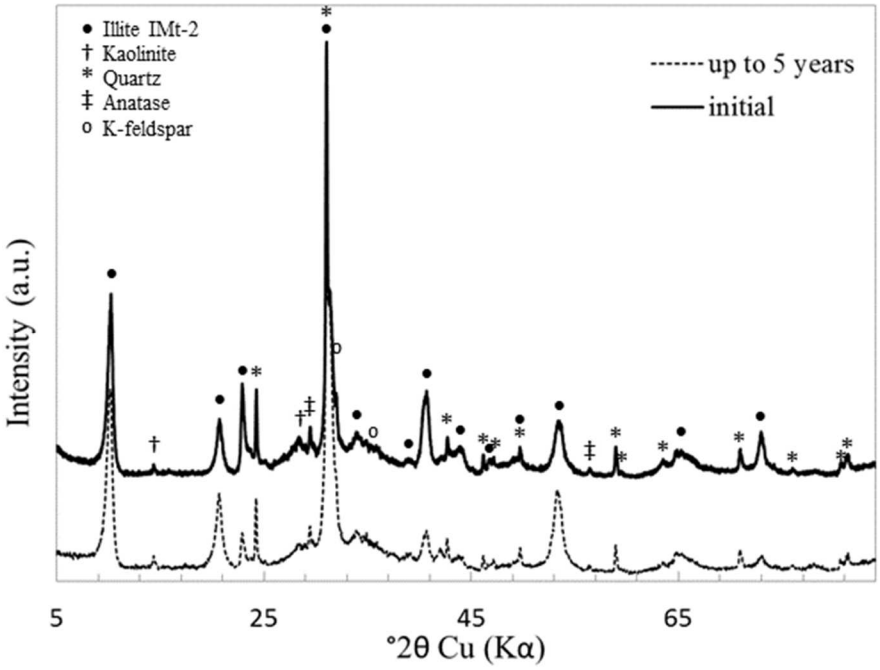

Figure 8 – X-ray diffractometer of illite random powder at initial state and after 5 years of interaction

For the longest reaction times, final saturation indexes are reported in Table 9 for each clay mineral and they have been represented also on Figure 9, at 25 and 40°C. For kaolinite, the indexes indicate equilibrium achievement after 7 years at 25°C while at 40°C after 2 years, a small departure from equilibrium is observed. Illite would have reach equilibrium after 5 years. MX-80 smectite is also reaching equilibrium.

On the other hand, vermiculite and especially chlorite display strong departure from equilibrium. The saturation index calculated and reported in Tables 7 and 8 are clearly decreasing (in absolute value) with time, indicating a tendency to reach equilibrium. But the evolution is processing at a considerably slower rate than for aforementioned clay minerals. Kaolinite, illite, MX-80 smectite and chlorite dissolution rates are reported in the database compiled by (Marty et al., 2015). To compare the different rate, we are considering the value of the kinetic constant for the neutral pH domain, at 25°C:

- Kaolinite $k^{neutral}_{25} = 8\ 10^{-13}$ mol.g^{-1}.s^{-1}
- Illite $k^{neutral}_{25} = 5\ 10^{-13}$ mol.g^{-1}.s^{-1}
- Smectite MX-80 $k^{neutral}_{25} = 1\ 10^{-14}$ mol.g^{-1}.s^{-1}
- Chlorite $k^{neutral}_{25} = 5\ 10^{-17}$ mol.g^{-1}.s^{-1}

Chlorite dissolution rate is slower than the rate for other minerals, at least at 25°C. The verification could not be held for vermiculite because of a lack of dissolution data in the literature.

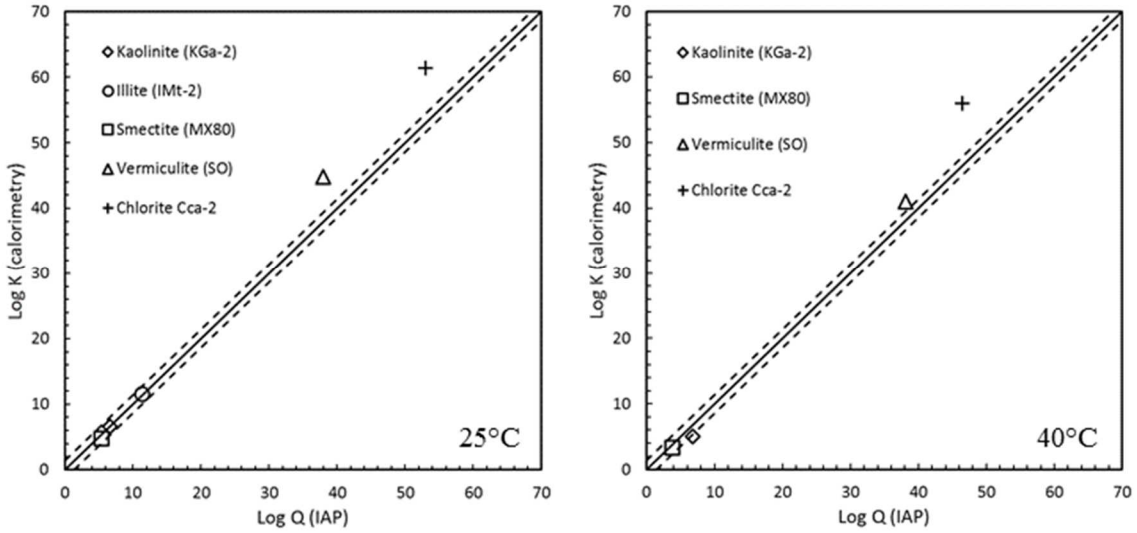

Figure 9 – Comparison of IAP values derived from solution experiments after 7 years with equilibrium constants calculated using measured thermodynamic properties (Gailhanou et al. 2012, 2013 and Blanc et al. 2014): a) at 25°C and b) at 40°C. Dotted lines correspond to uncertainty reported from the calorimetry measurements, for each phase

5.2 Comparison with literature

To discuss the solubility obtained in this work, we have realized a comparison with a selection of data from previous studies. In Table 10 are gathered experimental works from the literature devoted to illite, smectite (including beidellite) and chlorite. The selection was made using the following guidelines:

- No experiment using acidic solutions as starting media (as in Carson et al. (1976), Kittrick (1971a); Kittrick (1971c)
- No estimated value
- No experiment considering mixtures of minerals (with kaolinite or gibbsite as in Kittrick and Peryea (1988) or soil minerals as in Weaver et al. (1971)
- No experiment where the full list of dissolved element + pH is not reported
- Results obtained for theoretical end-member compositions are not selected.

The two last conditions suffered exceptions for iron-bearing minerals. Possibly because of the difficulty to analyse dissolve Fe, some previous authors have realized mixtures with iron-bearing phases (Kittrick, 1984a), with illite/goethite mixtures) or they have considered that dissolved iron was controlled by and iron hydroxide (Ferrihydrite for Misra and Upchurch (1976)). Such statement brings additional uncertainty but, since equilibrium was reached with respect to Ferrihydrite in some of our experiments (Vermiculite SO and Smectite MX-80), we consider the statement as reasonable. No estimates were selected and experiments where authors equilibrate mixtures of minerals were avoided, except for Kittrick (1984a) work, where the author mixed illite with goethite to avoid analyzing dissolved iron concentration for the solubility product calculation.

Table 10 – Selection of solubility experiment from previous literature and equilibrium calculated from dissolved elements and conditions specific to the studies

Reference	Type	Formula	Experiment conditions	Comments	logK (298.15 K)
Kittrick (1984b)	Illite (Beaver Bend)	$K_{0.53}(Al_{1.66}Fe_{0.2}Mg_{0.13})(Si_{3.62}Al_{0.39})O_{10}(OH)_2$	2.6 years ; with goethite ; continuous agitation	Formulas slightly modified (K content) to achieve neutrality ; logK averaged between runs without kaolinite and with dissolved Al ; dissolved Fe not reported	6.3
	Illite (Fithian)	$K_{0.64}(Al_{1.54}Fe_{0.29}Mg_{0.19})(Si_{3.51}Al_{0.49})O_{10}(OH)_2$			5.4
	Illite (Goose Lake)	$K_{0.59}(Al_{1.58}Fe_{0.24}Mg_{0.15})(Si_{3.65}Al_{0.35})O_{10}(OH)_2$			4.9
Reesman (1974a)	Illite (Fithian)	$(K_{0.6}Na_{0.05}Ca_{0.07})(Al_{1.20}Fe^{II}_{0.22}Fe^{III}_{0.45}Mg_{0.18})(Si_{3.46}Al_{0.54})O_{10}(OH)_2$	3.5 years ; analyses repeated several times ; in deionized water		1.7
	Illite (Grundy)	$(K_{0.69}Na_{0.03}Ca_{0.05})(Al_{1.56}Fe^{II}_{0.07}Fe^{III}_{0.04}Mg_{0.33})(Si_{3.58}Al_{0.42})O_{10}(OH)_2$			-2.0
	Illite (Marble Head)	$(K_{0.56}Na_{0.04})(Al_{1.50}Fe^{III}_{0.40}Mg_{0.24})(Si_{3.22}Al_{0.78})O_{10}(OH)_2$			6.6
	Illite (Rock Island)	$(K_{0.59}Na_{0.03}Ca_{0.03})(Al_{1.62}Fe^{II}_{0.08}Fe^{III}_{0.07}Mg_{0.26})(Si_{3.57}Al_{0.43})O_{10}(OH)_2$			6.3
Huang and Keller (1973b)	Illite (Beaver Bend)	$(K_{0.6}Na_{0.04})(Al_{1.43}Fe_{0.42}Mg_{0.16})(Si_{3.48}Al_{0.52})O_{10}(OH)_2$	102 days ; in deionized water	Calculations supposing equilibrium with ferrihydrite (as stated by the author) ; average between 3 experiments	10.3
	Illite (Fithian)	$(K_{0.59}Na_{0.02}Ca_{0.01})(Al_{1.54}Fe_{0.29}Mg_{0.23})(Si_{3.47}Al_{0.53})O_{10}(OH)_2$			0.9
	Montmorillonite SWy Clay spur	$(Na_{0.27}Ca_{0.10}K_{0.02})(Al_{1.52}Fe_{0.19}Mg_{0.22})(Si_{3.94}Al_{0.06})O_{10}(OH)_2$			6.5
	Montmorillonite Cheto	$(Na_{0.02}Ca_{0.19}K_{0.02})(Al_{1.52}Fe_{0.14}Mg_{0.33})(Si_{3.93}Al_{0.07})O_{10}(OH)_2$			8.7
(Misra and Upchurch, 1976)	Mg-Beidellite	$(Mg_{0.135}Ca_{0.01}Na_{0.07}K_{0.095})(Al_{1.41}Fe_{0.47}Mg_{0.205})(Si_{3.55}Al_{0.45})O_{10}(OH)_2$	60 days, shaken daily 8-10 hours; Probably in deionized water	Each LogK is averaged between three experiment	8.7
	K-Beidellite	$(Ca_{0.01}Na_{0.07}K_{0.365})(Al_{1.41}Fe_{0.47}Mg_{0.205})(Si_{3.55}Al_{0.45})O_{10}(OH)_2$			8.4
Aja and Darby Dyar (2002)	Fe-chlorite	$(Fe^{II}_{2.73}Fe^{III}_{0.30}Mg_{1.16}Al_{1.5})(Si_{2.82}Al_{1.18})O_{10}(OH)_8$	From 25 to 200°C ; with gibbsite or kaolinite	Formulas simplified removing minor elements ; LogK based on Gibbs energy	18
	Mg-chlorite	$(Al_{1.17}Fe^{II}_{0.58}Fe^{III}_{0.08}Mg_{4.21})(Si_{2.83}Al_{1.17})O_{10}(OH)_8$			48

As for kaolinite, Figure 10 displays a comparison of the LogK(T), up to 200°C. The equilibration at room temperature from this study is consistent with previous authors findings. The result at 40°C departs slightly from the main trend, while still remaining within the scattering of the experimental results.

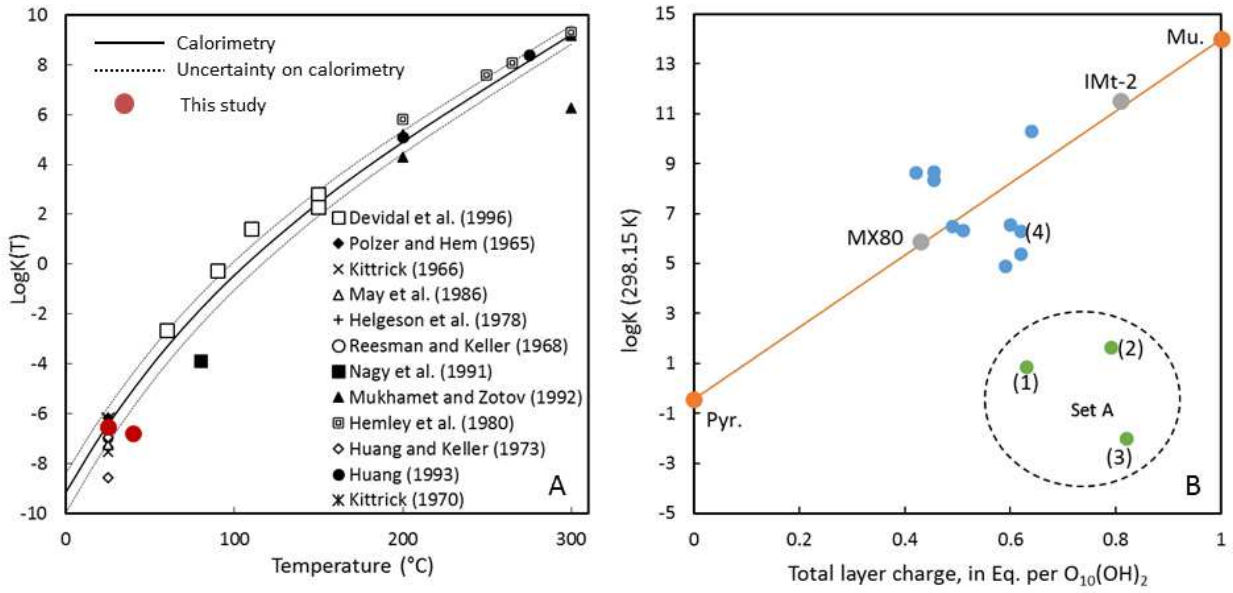

Figure 10 - Assessment of the results obtained in this work with respect to previous literature studies: A – Kaolinite equilibrium constant depending on temperature (modified from (Blanc et al., 2013)) ; B – Illites and smectites LogK (298.15 K) depending on the total charge deficit of the mineral. Values are from Table 10.

For illite and smectite, the comparison with our results is held on Figure 9-B where most of the equilibrium constants are located close to the Muscovite/pyrophyllite LogK line. Only few points are strongly departing from the main line (Set A in Figure 9-B). Among those, points 1 and 2 correspond to Fithian illite. Point 4 also corresponds to Fithian illite and the discrepancy with point 1 is close to 4.5 log units, whereas the structural formulas between both are very close. We can enhance the fact that Huang and Keller (1973a) experiments (point 1) were lasting only 102 days instead of 2.6 years for Kittrick (1984a) experiment (point 4). In addition, Huang and Keller (1973a) stated equilibrium with ferrihydrite, which was not achieved in our experiment on illite IMt-2. For point 3 (set A) from Reesman (1974b), few can be said, except that final pH seems quite low after 3.5 years of equilibration. In our case, the lowest pH where obtained for kaolinite and montmorillonite equilibration (between 4.5 to 5), up to close to 8 for illite. This could indicate difficulties to reach equilibrium, after Churchman and Jackson (1976). Based on 1 year equilibration at room temperature, (May et al., 1986) have discussed smectite stability. They report their results for pH, Si and Al activities, which does not allow calculating the logK for real smectite. Like Huang and Keller (1973a), they are stating for equilibrium with ferrihydrite to complete the set of activities. The point is questionable and our results indicates that equilibration solution can be at equilibrium with ferrihydrite but it is not always the case, as for Illite IMt-2 in this work. Approximating solutions composition to extract solubility products or equilibrium constant remains a tricky exercise. Another point in the work proposed by May et al. (1986) is equilibrium achievement hindered by amorphous hydroxide precipitation. The Gibbs phase rule does not prevent smectite to be at equilibrium with solution, while aluminium hydroxide is present. In geochemical modelling, the local equilibrium hypothesis, based on the Gibbs phase rule and the mass action law (Appelo and Postma, 1993), implies that several minerals can be

simultaneously at equilibrium with the solution provided to not overcome the degrees of freedom allowed by the Gibbs Phase Rule. Precipitation of aluminium hydroxide would modify the activities of Al aqueous species but this alone will not prevent smectite to reach equilibrium since the system possesses enough degrees of freedom. The comparison with equilibrium constants obtained in higher temperature conditions (as for muscovite and pyrophillite in Figure 9-B) or calculated from calorimetric measurements can provide less ambiguous ways to assess the equilibrium achievement for clay minerals at room temperature, as is displayed in this work.

For chlorites, we obtained an equilibrium constant logK (298.15 K) = 53 rather close from the result obtained by Aja and Dyar (2002) for the Mg-rich phase. The difference is much higher for the Fe-rich phase (logK = 18, (Aja and Dyar, 2002)). Such scattering is difficult to interpret, also given the scarcity of the data and the large composition domains of chlorites. It does not prove the attainment of equilibrium in our experiment. No reference could be found in the literature to compare results for Vermiculite.

5.3 Synthesis

In the experiments reported in this work, the results obtained depend on the composition of the clay minerals. For Al-rich, dioctahedral minerals, equilibrium could be achieved, from super saturation, within the span of the experiment duration. Equilibrium constant compare well with the calculation based on calorimetry measurements (Table 9). An exception is the results for kaolinite KGa-2 for which the saturation index was close to 0.2 at 25°C indicating equilibrium achievement while it reached +1.7 at 40°C, for an unknown reason. Saturation index found for smectite MX-80 reaches 0.50 at 40°C after 2 years and -0.1 for illite IMt-2 at 25°C after 5 years. Plotted against total layer charge, equilibrium constant do align consistently with results from the literature along a muscovite-pyrophyllite line.

The situation is different for the Fe-Mg-bearing clay minerals vermiculite SO and chlorite CCa-2. For both minerals, equilibrium is reached via dissolution (under saturation). The vermiculite saturation index after 2 years at 40°C reaches -2.93 ± 2.20. Equilibrium is not reached but the departure is not that large, given the uncertainty for both calorimetry and solution measurements. Given the evolution of the IAP with time displayed in Table 7, longer experiments could have reach equilibrium, at least at 40°C. For chlorite CCa-2, the final saturation index after 7 years at 25°C is -8.35, which is significantly far from equilibrium and calorimetric measurements are not verified is that case. Chlorite forms at higher temperatures than the other minerals considered here (Vidal et al., 2005). Their behavior could be similar to that of other types of minerals in that case (pyroxenes, amphiboles, micas), and their equilibrium at 25°C will depends on dissolution rate which is quite low for chlorite (Marty et al., 2015), at least at room temperature.

Eventually, to discuss the stability of clay minerals in contact with a solution we are referring to the mass action law, providing to this equation the full list of dissolved element, issued from chemical analyses. For complex compositions, a geochemical code has been used to avoid approximations in addressing activities from concentrations and activities were assigned with stoichiometric coefficients corresponding to the composition of the natural minerals. The comparison is held with equilibrium constants obtained experimentally with an independent method, using calorimetry measurements.

6. Conclusion

The document presents solution experiments, conducted on clay minerals and whose resulting IAP were compared to equilibrium constants calculated from thermodynamic properties directly measured by calorimetry.

The experimental design at 25°C was first refined in order to limit evaporation over the seven years of the experiments and to control the analytical results. Experiments at higher temperature (40°C) were also conducted with the goal of boosting the dissolution rate for the clay minerals and reduce the equilibrium attainment time. The experiment was performed for the following 5 clay minerals: kaolinite KGa-2, smectite MX-80, illite IMt-2, vermiculite SO and ripidolite Cca-2.

Among the 5 clays, equilibrium was reached for kaolinite, illite and smectite and results compare well with previous studies, considering a selection of literature works. From this point of view, this work enhances the need to consider all the dissolved element for IAP calculations, without approximation stating for equilibrium with other secondary phases.

For vermiculite and especially chlorite, equilibrium was still not reached, even after seven years at 25°C. Even if calculated IAP evolved toward equilibrium with time, quite slow dissolution seem to hinder equilibrium achievement, even attempting to boost dissolution rate by increasing temperature to 40°C. For such minerals, the lack of equilibrium solution experiment is another limit to correctly assess the validity of our results with respect to a broader set of works.

ACKNOWLEDGEMENTS

Financial support from the French National Radioactive Waste Management Agency (ANDRA) and from the French Geological Survey (BRGM) is gratefully acknowledged. We especially acknowledge our late colleague and friend Eric Giffaut who created and supported the Thermochimie database.

7. References

Aja, S.U., 1995. Thermodynamic Properties of Some 2/1 Layer Clay-Minerals from Solution-Equilibration Data. European Journal of Mineralogy 7, 325-333.

Aja, S.U., Darby Dyar, M., 2002. The stability of Fe–Mg chlorites in hydrothermal solutions—I. Results of experimental investigations. Applied Geochemistry 17, 1219-1239.

Aja, S.U., Dyar, M.D., 2002. The stability of Fe-Mg chlorites in hydrothermal solutions - I. Results of experimental investigations. Applied Geochemistry 17, 1219-1239.

Aja, S.U., Rosenberg, P.E., Kittrick, J.A., 1991a. Illite Equilibria in Solutions .1. Phase-Relationships in the System K2o-Al2o3-Sio2-H2o between 25 and 250-Degrees-C. Geochimica Et Cosmochimica Acta 55, 1353-1364.

Aja, S.U., Rosenberg, P.E., Kittrick, J.A., 1991b. Illite Equilibria in Solutions .2. Phase-Relationships in the System K2o-Mgo-Al2o3-Sio2-H2o. Geochimica Et Cosmochimica Acta 55, 1365-1374.

Appelo, C.A.J., Postma, D., 1993. Geochemistry, groundwater and pollution. Balkema, Rotterdam.

Bauer, A., Berger, G., 1998. Kaolinite and smectite dissolution rate in high molar KOH solutions at 35 degrees and 80 degrees C. Applied Geochemistry 13, 905-916.

Blanc, P., Gailhanou, H., Rogez, J., Mikaelian, G., Kawaji, H., Warmont, F., Gaboreau, S., Grangeon, S., Grenèche, J.-M., Vieillard, P., Fialips, C., Giffaut, E., Gaucher, E., Claret, F., 2014a. Thermodynamic properties of chlorite and berthierine derived from calorimetric measurements. Physics and Chemistry of Minerals 41, 603-615.

Blanc, P., Gailhanou, H., Rogez, J., Mikaelian, G., Kawaji, H., Warmont, F., Gaboreau, S., Grangeon, S., Grenèche, J.-M., Vieillard, P., Fialips, C.I., Giffaut, E., Gaucher, E.C., Claret, F., 2014b. Thermodynamic properties of chlorite and berthierine derived from calorimetric measurements. Physics and Chemistry of Minerals 41, 603-615.

Blanc, P., Lassin, A., Piantone, P., Azaroual, M., Jacquemet, N., Fabbri, A., Gaucher, E.C., 2012. Thermoddem: A geochemical database focused on low temperature water/rock interactions and waste materials. Applied Geochemistry 27, 2107-2116.

Blanc, P., Vieillard, P., Gailhanou, H., Gaboreau, S., 2013. Chapter 6 - Thermodynamics of Clay Minerals, in: Bergaya, F., Lagaly, G. (Eds.), Developments in Clay Science. Elsevier, pp. 173-210.

Cama, J., Ganor, J., Ayora, C., Lasaga, C.A., 2000. Smectite dissolution kinetics at 80 degrees C and pH 8.8. Geochimica Et Cosmochimica Acta 64, 2701-2717.

Carroll-Webb, S.A., Walther, J.V., 1988. A surface complex reaction model for the pH-dependence of corundum and kaolinite dissolution. Geochimica & Cosmochimica Acta, 2609-2623.

Carson, C.D., Kittrick, J.A., Dixon, J.B., Mckee, T.R., 1976. Stability of Soil Smectite from a Houston Black Clay. Clays and Clay Minerals 24, 151-&.

Chipera, S.J., Bish, D.L., 2001. Baseline studies of the clay minerals society source clays: powder X-ray diffraction analyses. Clays and Clay Minerals 49, 398-409.

Churchman, G.J., Jackson, M.L., 1976. Reaction of montmorillonite with acid aqueous solutions: solute activity control by a secondary phase. Geochimica et Cosmochimica Acta 40, 1251-1259.

Danzer, K., 2007. Analytical chemistry : theorical and mineralogical fundamentals, in: Springer (Ed.), p. 315.

Devidal, J.L., Dandurand, J.L., Gout, R., 1996. Gibbs free energy of formation of kaolinite from solubility measurement in basic solution between 60 and 170 degrees C. Geochimica Et Cosmochimica Acta 60, 553-564.
Devidal, J.L., Schott, J., Dandurand, J.L., 1997. An experimental study of kaolinite dissolution and precipitation kinetics as a function of chemical affinity and solution composition at 150 degrees C, 40 bars, and pH 2, 6.8, and 7.8. Geochimica Et Cosmochimica Acta 61, 5165-5186.
Gailhanou, H., Blanc, P., 2007. Thermochimie : Acquisition des propriétés thermodynamiquessur une saponite et révision des données sur les minéraux argileux., BRGM RP 55925 FR.
Gailhanou, H., Blanc, P., Rogez, J., Mikaelian, G., Horiuchi, K., Yamamura, Y., Saito, K., Kawaji, H., Warmont, F., Grenèche, J.-M., Vieillard, P., Fialips, C.I., Giffaut, E., Gaucher, E.C., 2013. Thermodynamic properties of saponite, nontronite, and vermiculite derived from calorimetric measurements. American Mineralogist 98, 1834-1847.
Gailhanou, H., Rogez, J., van Miltenburg, J.C., van Genderen, A.C.G., Greneche, J.M., Gilles, C., Jalabert, D., Michau, N., Gaucher, E.C., Blanc, P., 2009. Thermodynamic properties of chlorite CCa-2. Heat capacities, heat contents and entropies. Geochimica Et Cosmochimica Acta 73, 4738-4749.
Gailhanou, H., van Miltenburg, J.C., Rogez, J., Olives, J., Amouric, M., Gaucher, E.C., Blanc, P., 2007. Thermodynamic properties of anhydrous smectite MX-80, illite IMt-2 and mixed-layer illite-smectite ISCz-1 as determined by calorimetric methods. Part I: Heat capacities, heat contents and entropies. Geochimica Et Cosmochimica Acta 71, 5463-5473.
Gailhanou, H., Vieillard, P., Blanc, P., Lassin, A., Denoyel, R., Bloch, E., De Weireld, G., Gaboreau, S., Fialips, C.I., Madé, B., Giffaut, E., 2017. Methodology for determining the thermodynamic properties of smectite hydration. Applied Geochemistry 82, 146-163.
Giffaut, E., Grivé, M., Blanc, P., Vieillard, P., Colas, E., Gailhanou, H., Gaboreau, S., Marty, N., Madé, B., Duro, L., 2014. Andra thermodynamic data for performance assessment: Termochimie. Applied Geochemistry, accepted manusript.
Hofmann, H., Bauer, A., Warr, L.N., 2004. Behavior of smectite in strong salt brines under conditions relevant to the disposal of low- to medium-grade nuclear waste. Clays and Clay Minerals 52, 14-24.
Huang, W.H., Keller, W.D., 1973a. Gibbs free energies of formation calculated from dissolution data using specific mineral analyses. III. Clay minerals. American Mineralogist 58, 1023-1028.
Huang, W.H., Keller, W.D., 1973b. Gibbs free energy of formation calculated from dissolution data using specific mineral analyses. American Mineralogist 58, 1023-1028.
Kinniburgh, D., Cooper, D., 2011. PhreePlot: Creating graphical output with PHREEQC.
Kittrick, J., 1971a. Stability of Montmorillonites: II. Aberdeen Montmorillonite 1. Soil Science Society of America Journal 35, 820-823.
Kittrick, J.A., 1966. Free energy of formation of kaolinite from solubility measurements. American Mineralogist 51, 1457-1466.
Kittrick, J.A., 1971b. stability of Montmorillonites : I Belle Fourche and Clay Spur Montmorillonites. Soil Science society of America Proceedings 35, 140-145.
Kittrick, J.A., 1971c. Stability of Montmorillonites: I. Belle Fourche and Clay Spur Montmorillonites1. Soil Science Society of America Journal 35.

Kittrick, J.A., 1984a. Solubility Measurements of Phases in 3 Illites. Clays and Clay Minerals 32, 115-124.
Kittrick, J.A., 1984b. Solubility measurements of phases in three illites. Clays and Clay Minerals 32, 115-124.
Kittrick, J.A., Peryea, F.J., 1988. Experimental Validation of the Monophase Structure Model for Montmorillonite Solubility. Soil Science Society of America Journal 52, 1199-1201.
Kohler, S.J., Bosbach, D., Oelkers, E.H., 2005. Do clay mineral dissolution rates reach steady state? Geochimica Et Cosmochimica Acta 69, 1997-2006.
Kriaa, A., Hamdi, N., Srasra, E., 2009. Proton Adsorption and Acid-Base Properties of Tunisian Illites in Aqueous Solution. Journal of Structural Chemistry 50, 273-287.
Lasaga, A.C., 1998. Kinetic theory in the Earth Sciences, in: Press, P.U. (Ed.).
Marty, N.C.M., Cama, J., Sato, T., Chino, D., Villiéras, F., Razafitianamaharavo, A., Brendlé, J., Giffaut, E., Soler, J.M., Gaucher, E.C., Tournassat, C., 2011. Dissolution kinetics of synthetic Na-smectite. An integrated experimental approach. Geochimica et Cosmochimica Acta 75, 5849-5864.
Marty, N.C.M., Claret, F., Lassin, A., Tremosa, J., Blanc, P., Madé, B., Giffaut, E., Cochepin, B., Tournassat, C., 2015. A database of dissolution and precipitation rates for clay-rocks minerals. Applied Geochemistry 55, 108-118.
May, H.M., Klnniburgh, D.G., Helmke, P.A., Jackson, M.L., 1986. Aqueous dissolution, solubilities and thermodynamic stabilities of common aluminosilicate clay minerals: Kaolinite and smectites. Geochimica Et Cosmochimica Acta 50, 1667-1677.
Metz, V., Amram, K., Ganor, J., 2005. Stoichiometry of smectite dissolution reaction. Geochimica Et Cosmochimica Acta 69, 1755-1772.
Misra, U.K., Upchurch, W.J., 1976. Free Energy of Formation of Beidellite from Apparent Solubility Measurements. Clays and Clay Minerals 24, 327-331.
Oelkers, E.H., Schott, J., Devidal, J.-L., 1994. The effect of aluminum, pH, and chemical affinity on the rates of aluminosilicate dissolution reactions. Geochimica et Cosmochimica Acta 58, 2011-2024.
Parkhurst, D.L., 1995. User´s guide to PHREEQC- A computer program for speciation, reaction-path, advective-transport,and inverse geochemical calculations. U.S. Department of the Interior, Lakewood, Co.
Reesman, A., 1974a. Aqueous dissolution studies of illite under ambient conditions. Clays and Clay Minerals 22, 443-454.
Reesman, A.L., 1974b. Aqueous dissolution studies of illite under ambient conditions. Clays and Clay Minerals 22, 443-454.
Reesman, A.L., Keller, W.D., 1968. Aqueous solubility studies of high alumina and clay minerals. The American Mineralogist 53, 929-942.
Sato, T., Kuroda, M., Yokoyama, S., Fukushi, K., Tanaka, T., Nakayama, S., 2003. Mechanism and kinetics of smectite dissolution under alkaline conditions. Geochimica Et Cosmochimica Acta 67, A415-A415.
Tournassat, C., Davis, J.A., Chiaberge, C., Grangeon, S., Bourg, I.C., 2016. Modeling the Acid–Base Properties of Montmorillonite Edge Surfaces. Environmental Science & Technology 50, 13436-13445.
Tournassat, C., Ferrage, E., Poinsignon, C., Charlet, L., 2004. The titration of clay minerals II. Structure-based model and implications for clay reactivity. Journal of Colloid and Interface Science 273, 234-246.
Vidal, O., Parra, T., Vieillard, P., 2005. Thermodynamic properties of the Tschermak solid solution in Fe-chlorite: Application to natural examples and possible role of oxidation. American Mineralogist 90, 347-358.

Vieillard, P., Gailhanou, H., Lassin, A., Blanc, P., Bloch, E., Gaboreau, S., Fialips, C.I., Made, B., 2019. A predictive model of thermodynamic entities of hydration for smectites: Application to the formation properties of smectites. Applied Geochemistry 110, 104423.
Weaver, C.E., Beck, K.C., 1971. Clay water diagenesis during burial: How mud becomes gneiss. Geological Society of America Special Paper 134, 1-96.
Weaver, R.M., Jackson, M.L., Syers, J.K., 1971. Magnesium and Silicon Activities in Matrix Solutions of Montmorillonite-Containing Soils in Relation to Clay Mineral Stability1. Soil Science Society of America Journal 35, 823-830.
Wieland, E., Stumm, W., 1992. Dissolution kinetics of kaolinite in acid aqueous solutions at 25°C. Geochimica & Cosmochimica Acta 56, 3339-3355.
Xie, Z., Walther, J.V., 1992. Incongruent dissolution and surface area of kaolinite. Geochimica et Cosmochimica Acta 56, 3357-3363.